

Intramolecular Electron Transfer in Tetraammine(L)ruthenium(III)-Modified Manganocytchromes *c*

Ji Sun[†] and James F. Wishart*

Department of Chemistry, Brookhaven National Laboratory,
Upton, New York 11973

Received September 13, 1997

Cytochrome *c* is a small, water-soluble heme protein which shuttles an electron between two membrane-bound proteins in the respiratory chain of mitochondria. Its function as a facile, reversible redox partner has led to its use in numerous investigations of intra- and interprotein electron-transfer reactions. Some of these investigations employed the attachment of redox-active metal centers (such as ruthenium ammine^{1–7} or bipyridine^{7,8} complexes, pentacyanoferrate,⁹ or cobalt cage¹⁰ complexes) to residues on the surface of cytochrome *c* to (1) examine the effect of the intervening protein matrix on electron-transfer rates, (2) study the driving force dependence of electron transfer, or (3) initiate interprotein electron-transfer reactions within a protein–protein complex. In addition to studies of the native, iron-containing protein, electron-transfer reactions of the long-lived excited state of Zn-substituted cytochrome *c* have been extensively examined.^{7,11,12}

Recently, we reported¹³ intramolecular electron transfer measurements on pentaammineruthenium-modified, cobalt-substituted cytochrome *c*. Like native iron cytochrome *c*, the metal center in CoCyt *c* is six-coordinate and low-spin in both the II and III oxidation states. The reduction potential of CoCyt *c* is 0.40 V lower than that of FeCyt *c*, and the estimated self-exchange reorganization energy is much higher (2.4 eV vs 1.0 eV for FeCyt *c*).¹³ However, when the opposing effects of increased driving force and reorganization energy in the cobalt

case are accounted for, the activationless rate limit (indicative of the center-to-center electronic coupling) is nearly the same in the iron and cobalt cases.

This report presents our results on intramolecular electron transfer in ruthenium-modified, manganese-substituted cytochrome *c*, the only other derivative (aside from iron and cobalt) with two stable oxidation states. Unlike the other two, MnCyt *c* is high-spin and five-coordinate in both the Mn^{II} and Mn^{III} oxidation states.¹⁴ The reduction potential of MnCyt *c* was previously¹⁴ determined to be $+0.06 \pm 0.04$ V vs NHE by potentiometric titration. Despite the fact that reduced Mn^{II}Cyt *c* is rapidly oxidized by O₂, MnCyt *c* shows no activity with cytochrome *c* oxidase or reductase.¹⁴

Manganese-substituted horse heart cytochrome *c* was prepared according to the method of Dickinson and Chien.¹⁴ The absorption spectra we obtain for both oxidation states (Figure 1, Mn^{II} in the presence of excess sodium dithionite) agree with the published spectra.¹⁴ Mn^{III}Cyt *c* was derivatized at histidine-33 with (NH₃)₅Ru^{III} or *trans*-(NH₃)₄(L)Ru^{II}, L = pyridine or isonicotinamide, and purified by established procedures.^{1,15} Ruthenium-to-manganese ratios were determined by atomic absorption spectroscopy for each derivative (NH₃, 1.1; py, 0.85; isn, 0.87; uncertainty ~20%, concentrations 6–12 μM). Electropray mass spectra of (NH₃)₅Ru^{III}–Mn^{II}Cyt *c* showed a major peak at 12 540 Da, corresponding to the correctly modified species (see Supporting Information). In addition, sequential loss of ammonia ligands from the ruthenium complex under electropray conditions was indicated by a series of peaks of mass 12 540 – 17*n*, where *n* = 1–5. A small peak due to unmodified MnCyt *c* was seen around 12 355 Da. Electropray spectra of bona fide *trans*-(NH₃)₄(L)Ru^{II}–Mn^{III}Cyt *c* (L = pyridine or isonicotinamide) samples showed only native mass peaks at 12 358 Da. These ruthenium(II) complexes are apparently too labile to remain bound to histidine groups under electropray conditions, an effect also observed by others.¹⁶

MnCyt *c* is apparently electrochemically inactive at dipyriddy disulfide-coated gold electrodes that give good cyclic and differential pulse voltammetry results with FeCyt *c* and broad but clearly defined DPV peaks for CoCyt *c*. DPV scans of ruthenated MnCyt *c* samples show only the peak corresponding to the ruthenium couple and no peak assignable to MnCyt *c*. Examples for L = NH₃, py, and isn are given in the Supporting Information. The ruthenium couples appear at the same

[†] Present address: IGEN, Inc., 16020 Industrial Dr., Gaithersburg, MD 20877.

- (1) Sun, J.; Wishart, J. F.; Gardineer, M. B.; Cho, M. P.; Isied, S. S. *Inorg. Chem.* **1995**, *34*, 3301–3309.
- (2) Sun, J.; Isied, S. S.; Wishart, J. F. *Inorg. Chem.* **1995**, *34*, 3998–4000.
- (3) Wishart, J. F.; Sun, J.; Cho, M. P.; Su, C.; Isied, S. S. *J. Phys. Chem. B* **1997**, *101*, 687–693.
- (4) (a) Isied, S. S.; Worosila, G.; Atherton, S. J. *J. Am. Chem. Soc.* **1982**, *104*, 7659–7661. (b) Isied, S. S.; Kuehn, C.; Worosila, G. *J. Am. Chem. Soc.* **1984**, *106*, 1722–1726.
- (5) (a) Winkler, J. R.; Nocera, D. G.; Yocom, K. M.; Bordignon, E.; Gray, H. B. *J. Am. Chem. Soc.* **1982**, *104*, 5798–5800. (b) Nocera, D. G.; Winkler, J. R.; Yocom, K. M.; Bordignon, E.; Gray, H. B. *J. Am. Chem. Soc.* **1984**, *106*, 5145–5150.
- (6) Bechtold, R.; Gardineer, M. B.; Kazmi, A.; van Hemelryck, B.; Isied, S. S. *J. Phys. Chem.* **1986**, *90*, 3800–3804.
- (7) Winkler, J. R.; Gray, H. B. *Chem. Rev.* **1992**, *92*, 369–379.
- (8) Mines, G. A.; Bjerrum, M. J.; Hill, M. G.; Casimiro, D. R.; Chang, I.-J.; Winkler, J. R.; Gray, H. B. *J. Am. Chem. Soc.* **1996**, *118*, 1961–1965.
- (9) Moriera, I.; Sun, J.; Cho, M. O.-K.; Wishart, J. F.; Isied, S. S. *J. Am. Chem. Soc.* **1994**, *116*, 8396–8397.
- (10) Conrad, D. W.; Zhang, H.; Stewart, D. E.; Scott, R. A. *J. Am. Chem. Soc.* **1992**, *114*, 9909–9915.
- (11) Magner, E.; McLendon, G. *J. Phys. Chem.* **1989**, *93*, 7130–7134.
- (12) (a) Elias, H.; Chou, M. H.; Winkler, J. R. *J. Am. Chem. Soc.* **1988**, *110*, 429–434. (b) Meade, T. J.; Gray, H. B.; Winkler, J. R. *J. Am. Chem. Soc.* **1989**, *111*, 4353–4356. (c) Therien, M. J.; Selman, M.; Gray, H. B.; Chang, I.-J.; Winkler, J. R. *J. Am. Chem. Soc.* **1990**, *112*, 2420–2422.
- (13) Sun, J.; Su, C.; Wishart, J. F. *Inorg. Chem.* **1996**, *35*, 5893–5901.

- (14) (a) Dickinson, L. C.; Chien, J. C. W. *J. Biol. Chem.* **1977**, *252*, 6156–6162. (b) Purified metal-free H₂Cyt *c* (800 mg in 100mM NaPi, pH = 7.0) was washed five times by ultrafiltration (Amicon YM-3) with 50 mM Tris buffer (pH = 7.6). The repeated washing was to ensure that the solution was phosphate free, as the copresence of phosphate and KSCN would precipitate the protein. The H₂Cyt *c*/Tris solution was further washed three times with 2 M KSCN in 50 mM Tris buffer (pH = 7.8) and the final volume was adjusted to ~65 mL to make the H₂cyt *c* concentration around 1 mM. Mn(NO₃)₂·xH₂O (Alfa/Aesar Puratronic) was then added to the protein solution to give a final concentration of 10–15 mM. The solution was heated to 65 °C with a water bath for 15–20 min. The reaction mixture was centrifuged, and the desired supernate was washed by ultrafiltration with 50 mM Tris buffer (pH = 7.6) until it was KSCN free. The solution was concentrated and loaded on a CM-52 ion-exchange column and eluted with 100 mM NaPi, pH = 7.0. The yield of purified Mn^{III}Cyt *c* was 470 mg, or 59% based on metal-free H₂Cyt *c* and the published extinction coefficient (Mn^{III}: ε₃₇₀ = 84 400 M⁻¹ cm⁻¹).^{14a}
- (15) Yocom, K. M.; Shelton, J. B.; Shelton, J. R.; Schroeder, W. A.; Worosila, G.; Isied, S. S.; Bordignon, E.; Gray, H. B. *Proc. Natl. Acad. Sci. U.S.A.* **1982**, *79*, 7052–7055.
- (16) Fenwick, C. Private communication.

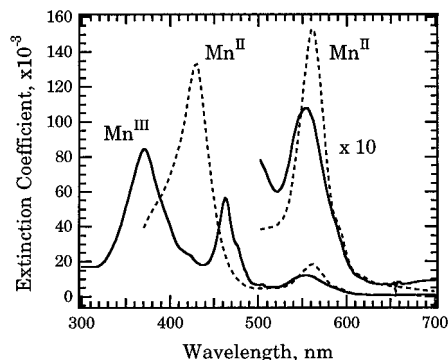


Figure 1. Absorption spectra of Mn^{III}Cyt *c* (solid line) and Mn^{II}Cyt *c* (dotted line) in 50 mM phosphate buffer, pH 7.0.

potentials observed in the corresponding ruthenated iron and cobalt horse heart cytochromes *c*. The apparent electrochemical inactivity may be related to the lack of reactivity of Mn^{II}Cyt *c* with cytochrome oxidase.¹⁴

The circular dichroism spectra of Mn^{II}Cyt *c* and Mn^{III}Cyt *c* are included in the Supporting Information. The Soret regions of the CD spectra show dramatic differences between the two oxidation states, in keeping with the absorption spectra. The fraction of helical content (f_H) within each of the protein derivatives can be calculated using the formula $[\theta]_{222} = -30300f_H - 2340$,^{17,18} where $[\theta]_{222}$ ($=[\theta]_{222}/104$ residues) is the mean residue ellipticity at 222 nm. Measurements of molar ellipticities for Mn^{III}Cyt *c*, (NH₃)₄Ru(L)-Mn^{III}Cyt *c* (L = NH₃, py, isn), and Mn^{II}Cyt *c* (-1.20×10^6 , -1.03×10^6 , -1.09×10^6 , -1.09×10^6 , and -1.84×10^6 deg cm²/dmol) result in calculated helicities of 30.4, 25.1, 26.9, 26.9, and 50.7%, respectively. A small decrease in helicity is observed upon addition of the pendant ruthenium group to manganocytocrome, as was observed in the case of Co^{III}Cyt *c*.¹³ The extremely high (51%) helicity estimated for Mn^{II}Cyt *c* (from two measurements) is remarkable and suggests a large degree of peptide backbone conformational change between the redox states; however, this method of helicity determination is subject to confounding factors such as spectral interference from the manganoheme prosthetic group.¹⁹

Preliminary measurements of the rate of reduction of Mn^{III}-Cyt *c* by CO₂^{•-} yield a rate constant of 2.1×10^8 M⁻¹ s⁻¹, which is larger than that of the reduction of Co^{III}Cyt *c* (1.4×10^8 M⁻¹ s⁻¹) but 9 times lower than that of Fe^{III}Cyt *c* (1.8×10^9 M⁻¹ s⁻¹). Oxidation of Mn^{II}Cyt *c* by the azide radical ($k = 4.6 \times 10^8$ M⁻¹ s⁻¹) is slower than that of Co^{II}Cyt *c* (8.0×10^8 M⁻¹ s⁻¹) and Fe^{II}Cyt *c* (1.3×10^9 M⁻¹ s⁻¹). Pendant (NH₃)₅Ru^{III/II}- groups are reduced by CO₂^{•-} with a rate constant^{4b} of $\sim 3 \times 10^9$ M⁻¹ s⁻¹ and oxidized by the azide radical¹³ at $\sim 1 \times 10^9$ M⁻¹ s⁻¹.

Pulse radiolysis transient absorption spectroscopy at 430 nm, near the maximum of the Mn^{II}Cyt *c* Soret band, was used to measure electron-transfer rates. For all three ruthenium derivatives, the reactions were initiated by the oxidation of the fully reduced Ru^{II}Mn^{II} species by the azide radical, N₃[•], producing the Ru^{III}Mn^{II} intermediate which undergoes electron transfer to give the ultimate Ru^{II}Mn^{III} product. This is the same technique used to study electron transfer in the native iron and cobalt-substituted cytochromes *c*.^{1,3,13} For the (NH₃)₅Ru- derivative,

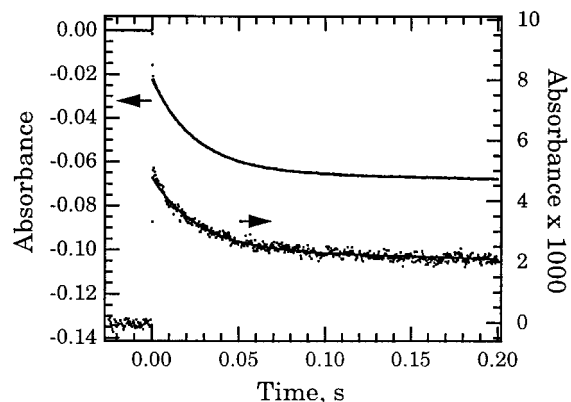


Figure 2. Pulse radiolysis transient absorption traces of intramolecular electron transfer in (NH₃)₅Ru-Mn Cyt *c* at 430 nm. Top trace, left axis: intramolecular ET initiated by oxidation of fully reduced Ru^{II}-Mn^{II} species by 0.34 μM N₃[•]. Conditions: 3.0 μM reduced ruthenated Mn Cyt *c*, 1 mM NaN₃, N₂O-saturated 50 mM phosphate buffer, pH = 7.0. Bottom trace, right axis: intramolecular ET initiated by reduction of fully oxidized Ru^{III}Mn^{III} species by 0.53 μM CO₂^{•-} radical. Conditions: 1.2 μM oxidized ruthenated Mn Cyt *c*, 100 mM sodium formate, N₂O-saturated 50 mM phosphate buffer, pH = 7.0.

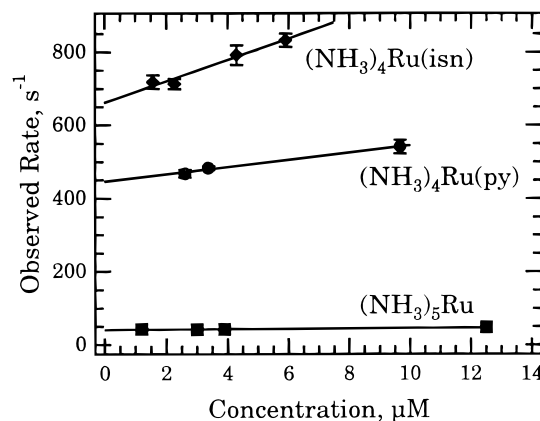


Figure 3. Observed electron-transfer rates in three ruthenium-modified manganocytocromes *c* as a function of concentration. Data are given in the Supporting Information.

it is also possible to follow electron transfer by the reduction of the Ru^{III}Mn^{III} species by CO₂^{•-},^{4b,20} although the dominance of the direct reduction of the ruthenium center results in a small signal from the Ru^{III}Mn^{II} intermediate.²¹ The results of the two methods are in complete agreement, as shown by Figure 2.

Electron-transfer rates were measured at several concentrations for each of the three ruthenium derivatives; the data are shown in Figure 3 and tabulated in the Supporting Information. The observed rate constants increase with concentration. We assign the intercepts of linear fits for each complex as the intramolecular electron-transfer rate constants and the slopes as the intermolecular rate constants. The results are presented in Table 1.

The rate of intramolecular electron transfer²² in (NH₃)₅Ru^{III}-Mn^{II}Cyt *c*, is 41 ± 1 s⁻¹ for a driving force of $\Delta G = -0.08$

(17) Snyder, F. W., Jr.; Chien, J. C. W. *J. Mol. Biol.* **1979**, *135*, 315–325.

(18) Chen, Y. H.; Yang, J. T.; Martinez, H. M. *Biochemistry* **1972**, *11*, 4120–4131.

(19) Myer, Y. P.; Pande, A. In *The Porphyrins*; Dolphin, D., Ed.; Academic Press: New York, 1978; Vol. 3, pp 271–322.

(20) This technique does not work well for the pyridine and isonicotinamide Ru^{III} complexes because they are prone to disproportionation and subsequent ligation changes and shifts to lower redox potentials.¹

(21) From the factor-of-2 difference between the initial and final absorbance values and the factor-of-15 difference in the rates of initial ruthenium and manganese reduction, it can be inferred that the equilibrium constant for Ru^{II}Mn^{III}/Ru^{III}Mn^{II} is on the order of 30 or more ($\Delta E \sim 90$ meV, $E_{\text{Mn Cyt}}$ between 40 and 70 mV vs NHE). This observation lowers the uncertainty in the upper bound of the reduction potential of Mn Cyt *c* reported in ref 14.

Table 1. Driving Forces, Rates, and Activation Parameters for Electron-Transfer Reactions of Ruthenium-Modified Manganocytocromes *c*^a

complex	ΔG° , ^b eV	k_{inter} , ^c M ⁻¹ s ⁻¹	k_{intra} , ^c s ⁻¹	$\Delta H_{\text{intra}}^\ddagger$, ^d kcal/mol	$\Delta S_{\text{intra}}^\ddagger$, ^d eu
(NH ₃) ₅ Ru-	-0.08	$(5 \pm 1) \times 10^5$	41 ± 1	4.8 ± 0.1 4.6 ± 0.3^e	-35.1 ± 0.3 -35.6 ± 1.1^e
(NH ₃) ₄ (py)Ru-	-0.31	$(9.9 \pm 0.1) \times 10^6$	446 ± 6	2.6 ± 0.1	-37.5 ± 0.3
(NH ₃) ₄ (isn)Ru-	-0.38	$(2.7 \pm 0.1) \times 10^7$	667 ± 2	1.5 ± 0.1	-40.4 ± 0.3

^a Conditions: N₂O-saturated 50 mM potassium phosphate, 1 mM NaN₃, pH = 7.0. ^b Driving forces estimated from the literature. Uncertainty 0.04 eV.^{1, 2, 14} ^c Calculated from observed rates at 25 °C as a function of concentration (Supporting Information). ^d Estimated from Eyring plots of data between 5 and 35 °C. See text. ^e Reductive method: N₂O-saturated 50 mM potassium phosphate, 100 mM sodium formate, pH = 7.0.

eV. Assuming for the sake of argument that the reorganization energy λ for MnCyt *c* is the same as that for FeCyt *c* (1.0 eV),²³ correcting the measured electron-transfer rate constant in the iron case (0.4 s^{-1} , $\Delta G = +0.125 \text{ eV}$)^{2,13} for the difference in driving force leads to an estimated rate of 23 s^{-1} , in fairly good agreement with the observed rate. However, due to the differences in coordination geometry between iron and manganese cytochromes in both oxidation states, it is unlikely that their reorganization energies are indeed similar. A great deal of further work is necessary to estimate the rate of MnCyt *c* self-exchange rate from cross-reactions in order to obtain a reliable value of λ for interpretation of the electron-transfer kinetics.

In the cases of ammineruthenium-derivatized iron and cobalt cytochromes, the variations of intramolecular electron-transfer rates with driving force obey Marcus-Hush theory very well.^{3,24} For MnCyt *c* the intramolecular and intermolecular rates increase with driving force by factors of 16.5 and 44, respectively, between the (NH₃)₅Ru- and (NH₃)₄Ru(isn)- derivatives, less than one may reasonably expect for a change of 0.30 eV. Estimated intramolecular electron-transfer rates based on FeCyt *c* values of $\lambda = 1.0 \text{ eV}$ and $k_{\text{max}} = 3.9 \times 10^5 \text{ s}^{-1}$,^{3,25} are 39, 3700, and 9000 s⁻¹, respectively, for the ammine, pyridine, and isonicotinamide derivatives, the last two estimates being about an order of magnitude faster than the observed rates. The possibility exists that for MnCyt *c* the actual electron-transfer step may not be rate limiting, particularly in the pyridine and isonicotinamide cases.^{26,27}

Activation parameters for all three derivatives (Table 1) were determined by measuring electron-transfer rates at 6, 16, 25, 35, and 45 °C using low (NH₃)₄Ru(L)-MnCyt *c* concentrations (1.2–3.0 μM) to minimize the contribution from the intermolecular rate. The Eyring plots (Supporting Information) are curved at higher temperatures, possibly due to increasing intermolecular contributions. Linear fits of the data between 6 and 35 °C were used to estimate the activation parameters. The activation entropies are much more negative for the MnCyt *c* derivatives than for the corresponding FeCyt *c* cases (–18 to

–22 eu)³ but comparable to those for CoCyt *c* (–36 to –39 eu).^{13,24} As in the cobalt case, a significant shortening of the axial Mn–His(18) bond upon oxidation may reduce conformational freedom in certain regions of the protein, leading to a decrease in entropy. A detailed analysis requires determination of the thermodynamic parameters in the CoCyt *c* and MnCyt *c* systems.

Acknowledgment. This research was carried out at Brookhaven National Laboratory under Contract DE-AC02-76CH00016 with the U.S. Department of Energy and supported by its Division of Chemical Sciences, Office of Basic Energy Sciences. The authors wish to thank Dr. Craig Fenwick and Prof. Ann English for the electrospray mass spectral analysis results.

Supporting Information Available: Table S-1, listing observed electron transfer rates in three ruthenium-modified manganocytocromes *c* as a function of concentration at 25 °C, and figures showing circular dichroism spectra of Mn^{II}Cyt *c* and Mn^{III}Cyt *c*, the electrospray mass spectrum of (NH₃)₅Ru^{III}-MnCyt *c*, differential pulse voltammograms of (NH₃)₅Ru-MnCyt *c*, (NH₃)₄Ru(py)-MnCyt *c*, and (NH₃)₄Ru(isn)-MnCyt *c*, and Eyring plots for intramolecular electron transfer in (NH₃)₅Ru-MnCyt *c* (by reduction with CO₂^{•-}) (NH₃)₅Ru-MnCyt *c* (by oxidation with N₃⁻), (NH₃)₅Ru(py)-MnCyt *c*, and (NH₃)₅Ru(isn)-MnCyt *c* (10 pages). Ordering information is given on any current masthead page.

IC971169P

(22) Properly speaking, the obtained rate constant is the sum of the forward and reverse rate constants; however, since the ratio k_f/k_r is on the order of 30 or more,²¹ k_r will be neglected.

(23) Marcus, R. A.; Sutin, N. *Biochim. Biophys. Acta* **1985**, *811*, 265–322.

(24) Sun, J.; Wishart, J. F.; van Eldik, R. Manuscript in preparation.

(25) The k_{max} value used here is appropriate for low-driving-force reactions of ruthenium ammine complexes bound to His33. If the k_{max} value of $2.6 \times 10^6 \text{ s}^{-1}$ obtained from ruthenium bipyridine complexes⁷ is used, the calculated rate constants would be an order of magnitude higher.

(26) If the (NH₃)₄(L)Ru^{III}-, L = pyr or isn, complexes had formed through inadvertent oxidation and then disproportionated in the presence of additional oxidant prior to the electron-transfer experiments, the resulting products would have lower potentials, which would reduce the ET driving force and lead to slower-than-expected rates.¹ However, these ruthenated manganocytocromes were handled with the same care to avoid Ru^{II} oxidation that worked successfully in previous iron^{1,3} and cobalt^{13,24} systems. In future work, we will deliberately allow the disproportionation reaction to proceed in order to investigate its effects on driving force and electron-transfer rates.

(27) (a) The ligation found in MnCyt *c* (five-coordinate with one axial histidine) is identical to that of *b*-type heme centers such as myoglobin and hemoglobin. Recently, electrochemical studies of manganese-substituted myoglobin in surfactant films have found evidence of a square redox scheme, with a slow rearrangement following reduction.^{27b} It is possible that conformational gating may limit the electron-transfer rates in these systems. (b) Farmer, P. J.; Lin, R.; Bayachou, M. *Comments Inorg. Chem.*, in press.